JOURNAL OF MATERIALS SCIENCE 33 (1998) 2817–2823

Enhancement of the ionic conductivity of poly(ethylene oxide) electrolyte film by polyaniline addition

JUN YANO*
Department of Engineering, University of East Asia, Ichinomiya-Gakuencho, Shimonoseki, Yamaguchi 751, Japan
Email: yano@po.pios.cc.toua-u.ac.jp

TAKAYUKI KOGA, SUMIO YAMASAKI
Department of Industrial Chemistry, Faculty of Engineering, Kyushu Sangyo University, Matsukadai, Higashi-Ku, Fukuoka 813, Japan

To improve the electrical conductivity of $LiClO_4$–poly(ethylene oxide) (PEO) complex, non-conductive polyaniline (NPANI) was employed as an additive. The electrical conductivity of the PEO–$LiClO_4$–NPANI electrolyte was at least ten times that of the original PEO–$LiClO_4$ electrolyte. The amine and/or imine nitrogen atoms in the NPANI polymer chain as well as the oxygen atoms in the PEO polymer chain attracted the Li^+ ions, and ion–dipole interaction occurred. The interaction enhanced the mobility of the ClO_4^- ions. The positively charged nitrogens were electronically stabilized in the entire polymer chain because NPANI had conjugated π electrons. The mechanism is unique and different from those of other polymer additives. It is the very first example in which NPANI was employed as the additive for the PEO solid electrolyte and in which NPANI was found to be an effective additive. In addition, the NPANI addition hardly affected the physical properties of the PEO matrix such as the glass transition temperature and the melting temperature.

1. Introduction

The discovery of ionic conductivity in alkali cation poly(ethylene oxide) (PEO) complexes [1] has greatly stimulated the development of electrochemical devices such as rechargeable batteries, electrochromic displays and sensors, because electrolytic-solution-free devices can be made. Numerous fundamental and technological studies on PEOs have been reported. Unfortunately, however, the technically justified level of 10^{-4}–10^{-3} S cm^{-1} at room temperature has not yet been achieved [2].

To obtain higher conductivity, we have three strategies: (1) surveying a variety of polymer systems other than PEOs; (2) modifications of the PEO system; (3) evaluation of various additives to PEOs. In strategy (1), many candidate polymers have been tested for solid electrolytes, and ionic conductivity has been found in the following polymers: poly(propylene oxide) [3], aliphatic polyesters [4], poly(β-propiolactone) [5] and polyimines [6]. On the other hand, a cross-linking technique of the PEO polymeric chains is employed as the modification of strategy (2). The cross-linking transforms crystalline PEO phases into amorphous phases. The amorphous phase mainly contributes towards the ionic conductivity of alkali cation PEO complexes, and the increase in the amorphous phases improves the electrical conductivity. Several successful examples of the strategy have been reported to date [7–16].

Nevertheless, the highest electrical conductivity obtained at room temperature only slightly exceeds 10^{-4} S cm^{-1} [10, 14, 16]. Although both strategy (1) and strategy (2) mainly aim to prepare more favourable polymer morphology for the ion transport of the salt in the polymer–electrolyte system, the enhancement of the electrical conductivity seems to have limitations.

We wish to employ strategy (3) in this paper. An appropriate additive is expected not only to improve the mechanical strength of the electrolyte and to give more favourable polymer morphology for the ion transport of the salt but also to promote ion transport by an electrostatic or electrophoretic effect of the additive. Some ceramic and polymer additives have been tested and several effective additives have been found. Among them, polymer additives containing hetero atoms in their polymeric backbones are attractive because the electrostatic force of the hetero atoms assists the dissociation of the alkali salts in the electrolytes. The blending of poly(vinylidene fluoride) with PEO–salt polymer electrolytes improves their ionic

---

*To whom all correspondence should be addressed.

0022–2461

conductivity [17]. The blending increases the amorphous phase and the dielectric constant of the medium. On the other hand, the blending of poly(2- or 4-vinylpyridine) also enhances the ionic conductivity of the PEO–$LiClO_4$ polymer electrolytes [18]. The enhancement is caused by the ion–dipole interaction of the Li^+ with the oxygen atoms of the PEO and the nitrogen atom of the pyridine units.

In this paper, we employ soluble non-conductive polyaniline (NPANI) as the candidate polymer additive with stronger ion–dipole interaction and higher dielectric constant. Polyaniline (PANI) is a typical electron-conductive polymer with conjugated π electrons. PANI has a high electrical conductivity only when it is protonated (i.e., doped by anions), and it is insoluble in any organic solvent [19]. The insolubility causes difficulties in homogeneous blending with PEO electrolytes. Although deprotonated PANI (i.e., NPANI), which is soluble in common organic solvents, shows no electrical conductivity, it is attractive for our objective because it has amine and/or imine nitrogen atoms in the polymeric backbone. Such nitrogen atoms are expected to attract the Li^+ ions in the PEO–$LiClO_4$ electrolyte and to enhance the mobility of the ClO_4^- ions. In this paper, we show that NPANI is an effective additive to enhance the ionic conductivity of the PEO–$LiClO_4$ electrolyte. We also suggest how NPANI functions in the ion transport inside the electrolyte.

2. Experimental procedure

2.1. Chemicals

Linear PEO (Aldrich; molecular weight, 100 000), acetonitrile (Wako Jun-yaku), pyridine (Wako Jun-yaku) and aniline (Wako Jun-yaku) were reagent grade and used without further purification. Special-grade anhydrous metal salts such as $LiClO_4$ (Wako Jun-yaku) were dried in a vacuum oven at 180 °C for 8 h and stored in a desiccator. NPANI was prepared using the literature method; PANI was prepared by chemical or electrochemical oxidation of aniline [19], and the PANI was further treated with NaOH solution [20]. The resulting NPANI was non-conductive and soluble in pyridine.

2.2. Preparation of poly(ethylene oxide)–$LiClO_4$–non-conductive polyaniline electrolyte film

All the PEO–$LiClO_4$–NPANI electrolyte films were easily prepared using the same method, except that the added amounts of the metal salt, PEO and NPANI were different. The NPANI-saturated pyridine solution was uniformly mixed with acetonitrile solution containing a metal salt such as $LiClO_4$. PEO was then dissolved in the mixture. After the mixture was cast on the Petri dish, the acetonitrile–pyridine solvent was removed from the mixture by vacuum drying, and a stable PEO–$LiClO_4$–NPANI electrolyte film was obtained. To dehydrate the obtained film, the film was vacuum dried at 75 °C for at least 2 days. Dry air was used to release the vacuum, and the film was immediately covered and stored in a desiccator prior to testing. The film thickness was around 0.5 mm. The detailed procedure is schematically depicted in Fig. 1.

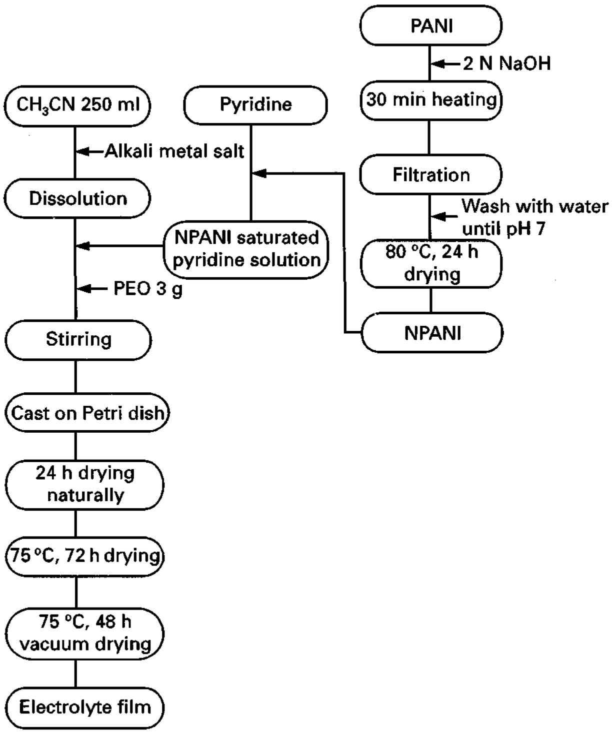

Figure 1 Schematic diagram of the preparation of the PEO–$LiClO_4$–NPANI electrolyte film.

2.3. Optimum added amount of $LiClO_4$ for poly(ethylene oxide) matrix

It is widely accepted that, the greater the amount of $LiClO_4$ salt added to the PEO matrix, the higher is the conductivity. Unfortunately, however, excessive addition of $LiClO_4$ makes the PEO–$LiClO_4$ electrolyte film sticky and the film loses its mechanical strength. The same behaviour was observed for our PEO–$LiClO_4$ film. To estimate the optimum amount of added $LiClO_4$, the mechanical strength was monitored for each PEO–$LiClO_4$ film with different $LiClO_4$ contents. The PEO–$LiClO_4$ film showed almost the same strength as the original PEO film without $LiClO_4$, unless the molar ratio of $LiClO_4$ to the PEO units, $[LiClO_4]/[EO\ unit]$, exceeds 0.07. The film became sticky above the ratio of 0.07, and it was not free standing at the ratio of 0.10. As a result, the ratio of the film used in this work was kept at 0.07.

2.4. Electrical conductivity

Conductivity measurements were carried out on the polymer electrolyte films held between two copper plate terminals, using both an Advantest R6142 direct-current source and an Advantest R6441 voltmeter. The film was penetrated by two copper pole terminals (0.8 mm in diameter) for voltage measurements at various constant currents. This arrangement is shown in Fig. 2. The bulk resistance, R, was derived from the current–voltage curve of the film where Ohm's law is obeyed. The electrical conductivity, σ, of

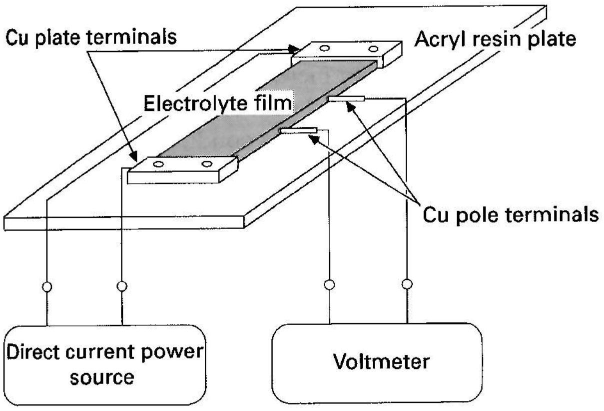

Figure 2 Schematic three-dimensional view of the apparatus for the conductivity measurement of the electrolyte film.

the film was calculated from R according to

$$\sigma = \frac{l}{A}\frac{1}{R} \qquad (1)$$

where l is the length of the film and A is the cross-sectional area of the film. In addition, the device shown in Fig. 2 was placed in an Oxford Instruments DN 1754 cryostat with an Oxford Instruments ITC 502 temperature controller when the relationship between σ and temperature was examined.

2.5. Differential scanning calorimetry

The thermal transitions of the polymer electrolyte films were measured with a Rigakudenki DSC 8230 differential scanning calorimeter, at a heating rate of 5 °C min^{-1}, in a dry nitrogen stream of 50 cm^3 min^{-1}. Before obtaining the thermograms, the sample was pre-heated in the differential scanning calorimeter cell at 120 °C for 5 min in the dry nitrogen stream to evaporate any condensed water on site. It was then cooled to 0 °C at a rate of 320 °C min^{-1}.

The glass transition temperatures, T_g, were obtained at the midpoints of the heat capacity changes, and the melting temperatures, T_m, were obtained at the maximum of the enthalpy endothermic peaks.

2.6. X-ray diffraction spectra

X-ray diffraction patterns were measured with a Rigakudenki RAD-IIIA X-ray diffractometer. The radiation used was Ni-filtered Cu$K\alpha$. The X-ray sample chamber was first dried with P_2O_5 powder overnight before a sample powder was inserted for measurement.

2.7. Absorption spectra

To examine the electronic state of NPANI in the polymer electrolyte films, the absorption spectra of the films containing NPANI were measured with a Nippon Bunko Ubest-55 spectrophotometer. For comparison, the absorption spectra of both the NPANI film and the PANI film were also measured. The electrode substrate where the PANI film was electrodeposited was a transparent indium tin oxide (ITO) plate. The NPANI film was obtained by the alkali treatment of the PANI film ITO plate.

2.8. X-ray photoelectron spectra

To examine the electronic interaction between NPANI and metal cation, the X-ray photoelectron spectra of the polymer electrolyte films were measured. The X-ray photoelectron spectra were recorded by an ESCA PHI 5400 (Perkin–Elmer Co.) spectrometer using a Mg$K\alpha$ anode with a power of about 400 W. The vacuum level during the measurement was lower than 10^{-9} Torr. The C 1s binding energy of 284.6 eV was used as the internal standard.

3. Results and discussion

3.1. Enhancement of the electrical conductivity by non-conductive polyaniline addition

Fig. 3 shows the relationship between the electrical conductivity, σ, of the PEO–$LiClO_4$–NPANI electrolyte and the added amount of NPANI. For comparison, the conductivity change with the $LiClO_4$ content is also shown for the PEO–$LiClO_4$ electrolyte without NPANI. As expected, σ uniformly increases with increasing $LiClO_4$ content. The PEO–$LiClO_4$ film showed almost the same mechanical strength as the original PEO film without $LiClO_4$, unless the molar ratio of the PEO unit to $LiClO_4$, [$LiClO_4$]/[EO unit] exceeds 0.07. Unfortunately, however, the film became sticky above the ratio of 0.07, and it was not free standing at the ratio of 0.10. Therefore, the film with the ratio of 0.07 was used as the sample for NPANI blending.

It is surprising that σ abruptly increases with increasing added amount of the NPANI, and σ is about one order higher than that of the original PEO electrolyte. Although it has been reported that several polymer additives such as polyvinylpyridines enhance the σ of PEO electrolytes [17, 18], the enhancement is much lower than that obtained with NPANI. This suggests that the enhancement of σ in the PEO–$LiClO_4$–NPANI electrolyte is caused by a different mechanism. This mechanism will be discussed in a later section.

3.2. Contribution of non-conductive polyaniline to ionic conductivity

To examine whether the enhanced conductivity due to the NPANI addition is a result of the electronic current of the additive NPANI, two experiments were carried out: σ measurements of the PEO–NPANI electrolyte film without $LiClO_4$, and observations of the temperature dependence of the PEO–$LiClO_4$–NPANI electrolyte films.

The electrical conductivity of the PEO–NPANI electrolyte film without $LiClO_4$ was found to be less than 10^{-7} S cm^{-1}. The negligible conductivity hardly increased even when the added amount of NPANI

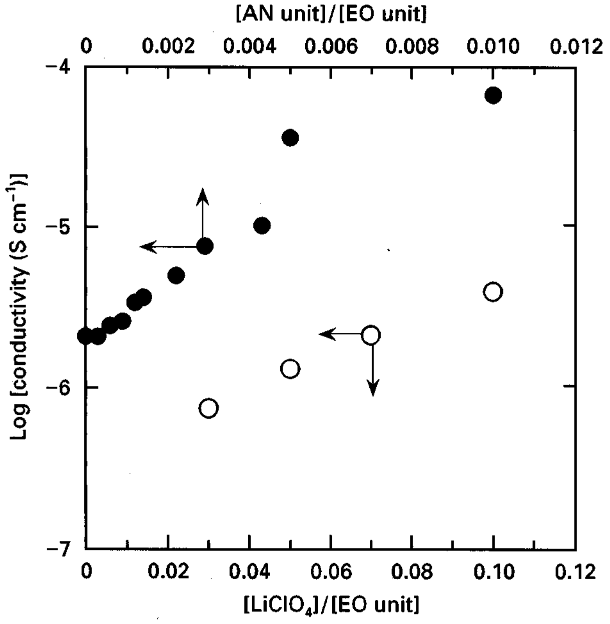

Figure 3 Change in the electrical conductivity, σ, of the PEO–NPANI electrolyte as the function of the added amount of $LiClO_4$ (○) and NPANI (●). The electrolyte sample having the molar ratio, $[LiClO_4]$/[EO unit], of 0.07 was used when NPANI was added. The measurements were carried out at 25 °C.

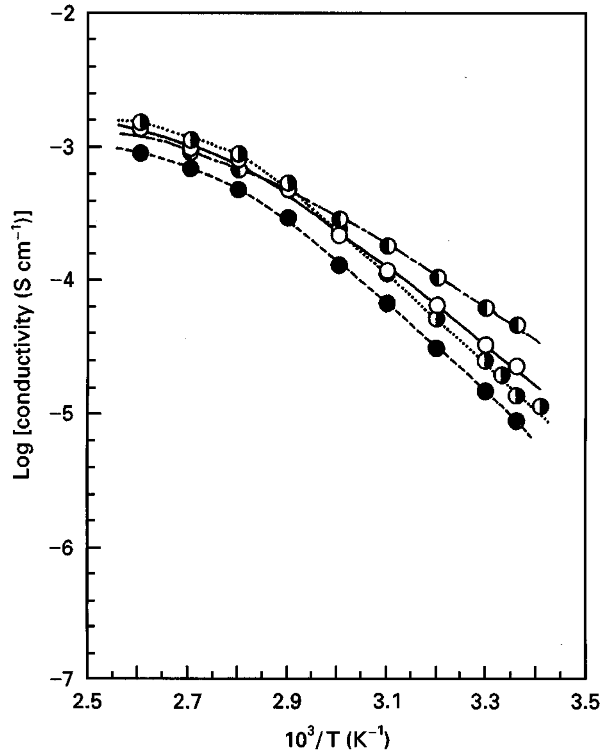

Figure 4 Arrhenius plots of the electrical conductivity, σ, for three PEO–$LiClO_4$–NPANI electrolyte films with different molar ratios, [AN unit]/[EO unit]. (◐), 0.00118; (○), 0.00236; (◑), 0.00472. The plots for the original PEO–$LiClO_4$ electrolyte film without NPANI (●) are also shown for comparison.

was increased. This excludes the contribution of the electronic current of NPANI from the enhanced conductivity. In other words, NPANI promotes ion transport inside the electrolyte film, although NPANI does not act as an electron conductor in the film.

Fig. 4 shows the Arrhenius plot of the electric conductivity of the PEO–$LiClO_4$–NPANI electrolyte films. The conductivity increased with increase in the molar ratio of the NPANI unit to the PEO unit, [AN unit]/[EO unit]. The highest conductivity of 1.58×10^{-3} S cm^{-1} appears for the film with [AN unit]/[EO unit] = 0.00472 at 100 °C. All the curves in Fig. 4 follow the Williams–Randel–Ferry [21] type of equation [4]

$$\log\left(\frac{\sigma(T)}{\sigma(T_g)}\right) = \frac{C_1(T - T_g)}{C_2 + (T - T_g)} \qquad (2)$$

implying that the electrical conductivity is due to the charge transport of Li^+ and/or ClO_4^- in the amorphous phase of the PEO matrix.

3.3. Role of non-conductive polyaniline in the poly(ethylene oxide)–$LiClO_4$–non-conductive polyaniline electrolyte

To examine the electronic state of NPANI in the PEO matrix, the optical absorption spectra of the PEO–$LiClO_4$–NPANI electrolyte films were monitored and compared with the original polyaniline films. The spectra are shown in Fig. 5. In the visible wavelength range, conductive anion-doped PANI has an absorption band around 790 nm, while non-conductive de-doped PANI, i.e., NPANI, has a band around 580 nm. These bands coincide in position with those reported elsewhere [22, 23].

It is interesting to find that the maximum absorption wavelength of NPANI in the film is about 70 nm larger than that of the original NPANI film. This shift leads to the conclusion that the NPANI in the film is electronically stabilized in the PEO matrix. The stabilization is probably due to the conjugated π electrons generated in NPANI by the Li^+ ions. The conjugated π electrons must not be expanded over the whole polymer chain because of the small wavelength shift of about 70 nm.

A proposed mechanism of the enhanced ion transport in the PEO–$LiClO_4$–NPANI electrolyte is schematically depicted in Fig. 6. The bond energy of $LiClO_4$ is weakened by the electrostatic attraction of the oxygens of the PEO polymer chain, and the ClO_4^- ions become mobile (Fig. 6a). When NPANI is added, the NPANI polymer chains become entangled in the PEO polymer chains. It is accepted for the PEO–polyvinylpyridine electrolytes that the lone pair of nitrogen electrons in the polymeric backbone attracts Li^+ and the ClO_4^- becomes more mobile because of ion–dipole interaction [17, 18]. This Li^+ attraction occurs more strongly in NPANI than in polyvinylpyridines because NPANI has conjugated π electrons. The positively charged nitrogens are electronically stabilized by the π electrons (Fig. 6c). The Li^+ attraction of the nitrogen atom of the NPANI polymer chain is smaller than that of the oxygen atom of the PEO polymer chain, and the ion–dipole interaction is much greater than that for polyvinylpyridines. In the PEO–NPANI electrolyte, therefore, the ion transport is greatly promoted.

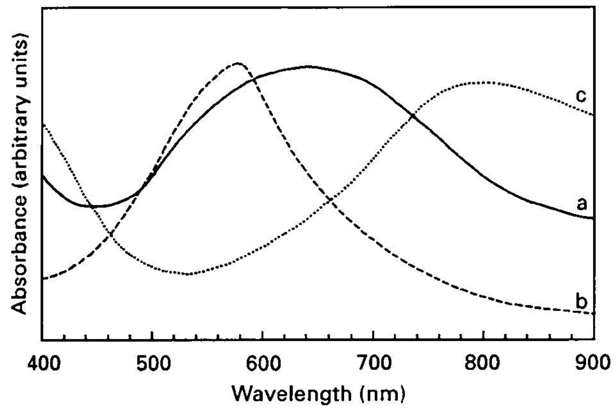

Figure 5 Optical absorption spectra of the PEO–LiClO$_4$–NPANI electrolyte film (curve a), the NPANI film (curve b) and the PANI film (curve c).

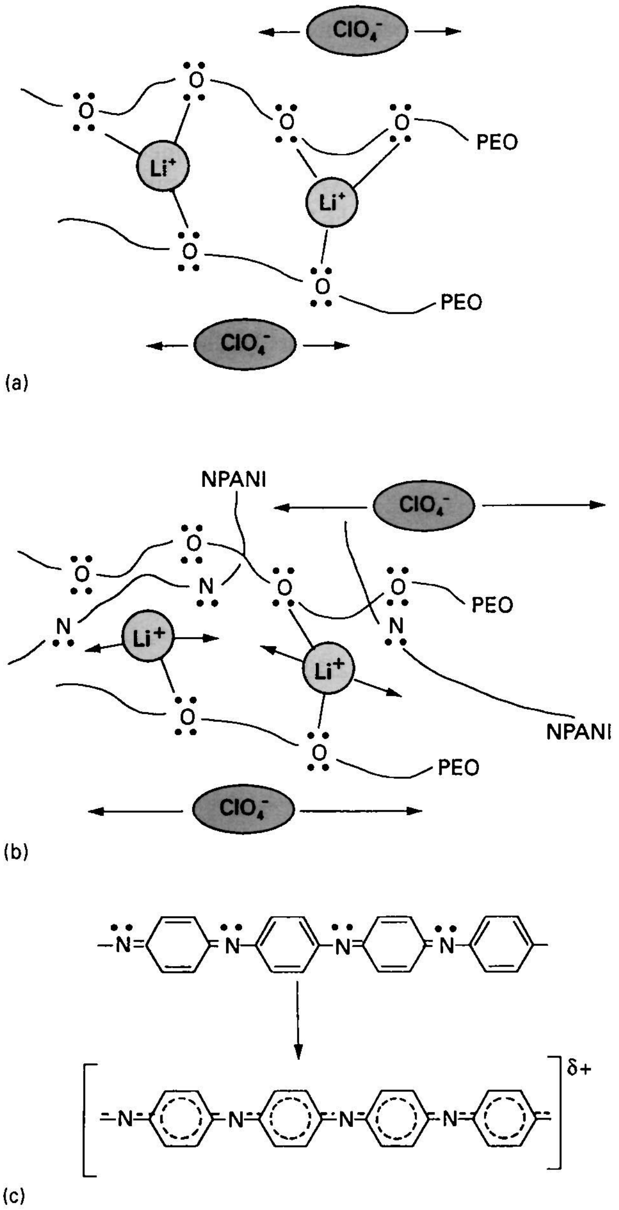

Figure 6 Proposed schematic expression for the enhanced ion transport of ClO$_4^-$ in the PEO–LiClO$_4$–NPANI electrolyte. (a) Li$^+$ attraction by the oxygen atoms of the PEO polymer chains. (b) Li$^+$ attraction by the nitrogen atoms of the NPANI polymer chains as well as the oxygen atoms of the PEO polymer chains. Ion–dipole interaction and enhancement of the ClO$_4^-$ ion transport in the electrolyte occurs. (c) Electronic stabilization of the positively charged NPANI.

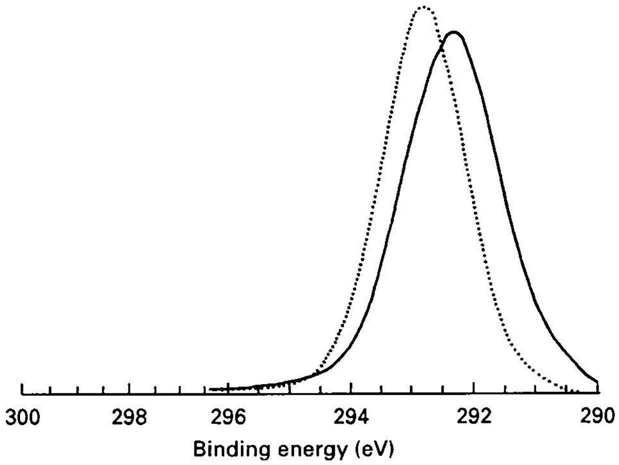

Figure 7 X-ray photoelectron spectra of K 1s for the PEO–LiClO$_4$ electrolyte film (···) and the PEO–LiClO$_4$–NPANI electrolyte film (———) ([KClO$_4$]/[EO unit] = 0.07; [AN unit]/[EO unit] = 0.004 72).

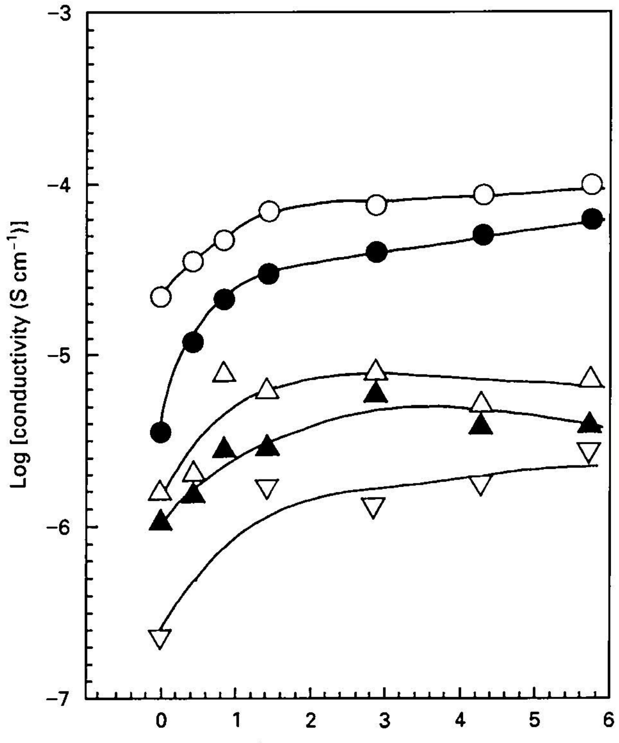

Figure 8 Logarithmic change in the electrical conductivity, σ, of five PEO–alkali metal salt–NPANI electrolytes as a function of the added amount of NPANI. The five alkali metal salts dissolved in each PEO matrix were LiBF$_4$ (○), LiClO$_4$ (●), LiCF$_3$SO$_3$ (△), LiBr (▲) and LiCl (▽). The electrolyte sample having the molar ratio, [alkali metal salt]/[EO unit], of 0.07 was used when NPANI was added. The measurements were carried out at 25 °C.

To obtain evidence of the above mechanism, the X-ray photoelectron spectra of the PEO–KClO$_4$ electrolyte film with and without NPANI were measured. The reason why KClO$_4$ was used here instead of LiClO$_4$ is that the X-ray photoelectron spectroscopy signals of the Li were too small to be detected because of the much lower selective factor of Li than those of other metal atoms. Fig. 7 shows the X-ray photoelectron spectra of K 1s of the PEO–KClO$_4$

electrolyte film with and without NPANI. The binding energy of K 1s is 292.84 eV, which becomes 292.47 eV when NPANI is added. On the other hand, the binding energies of O 1s and Cl 2p were almost constant within 0.05 eV for the PEO–$KClO_4$ electrolyte film with and without NPANI. Therefore, the 0.37 eV shift of K 1s strongly supports the mechanism shown in Fig. 6.

Indirect evidence of the mechanism in Fig. 6 was also obtained from the electric conductivity measurements for each PEO–NPANI film containing a different anion or cation. The conductivity was almost constant when other metal perchlorates such as $KClO_4$ and $NaClO_4$ were used instead of $LiClO_4$. On the other hand, the anions greatly influenced the conductivity (Fig. 8). The dissociation energies of the metal perchlorates are listed in Table I. Judging from Table I, the conductivity is enhanced according to the order of the dissociation energy. The Li^+ attraction of the NPANI occurs more frequently in the electrolyte with lower dissociation energy, and more ClO_4^- ions act as charge carriers. Thus, the above results strongly support the mechanism in Fig. 6.

TABLE I Dissociation energy, *D*, of alkali metal salts used

Alkali metal salt	*D* (kJ mol^{-1})
$LiBF_4$	699
$LiClO_4$	733
LiBr	807
LiCl	853

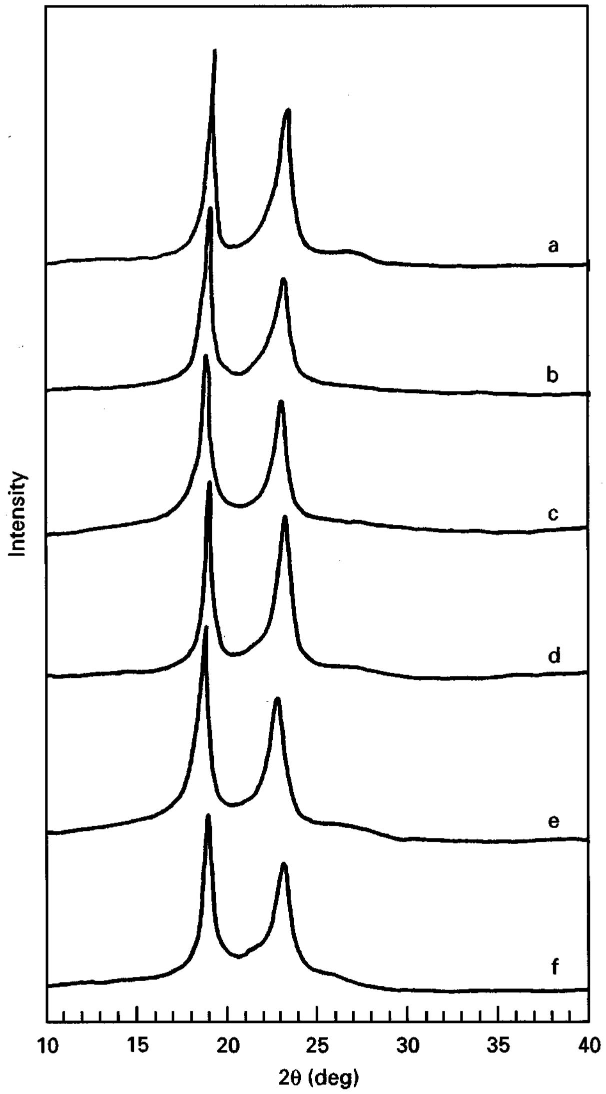

Figure 9 X-ray diffraction patterns of five PEO–$LiClO_4$–NPANI electrolytes with various [AN unit]/[EO unit] ratios. Curve b, 0.0012; curve c, 0.0022; curve d, 0.0043; curve e, 0.0059; curve f, 0.0118. The original PEO–$LiClO_4$ electrolyte without NPANI (curve a) is also shown for comparison.

3.4. X-ray diffraction and differential scanning calorimetry

Figure 9 shows the X-ray diffraction patterns of the PEO–$LiClO_4$–NPANI electrolyte films with different contents of NPANI. The original PEO, without any additive, is a crystalline polymer and has sharp diffraction peaks at $2\theta = 19.0°$ and $23.0°$ (Fig. 9, curve a). All five PEO–$LiClO_4$–NPANI electrolyte films show only two diffraction peaks at the same positions as those of the original PEO. No other peaks originating from crystalline $LiClO_4$ and from the formation of a new crystalline complex were observed, implying that $LiClO_4$ dissolves in the amorphous phase of the PEO matrix. In addition, the peak intensity is lowered by the NPANI addition. This leads to the conclusion that the addition of NPANI, as well as $LiClO_4$, assists

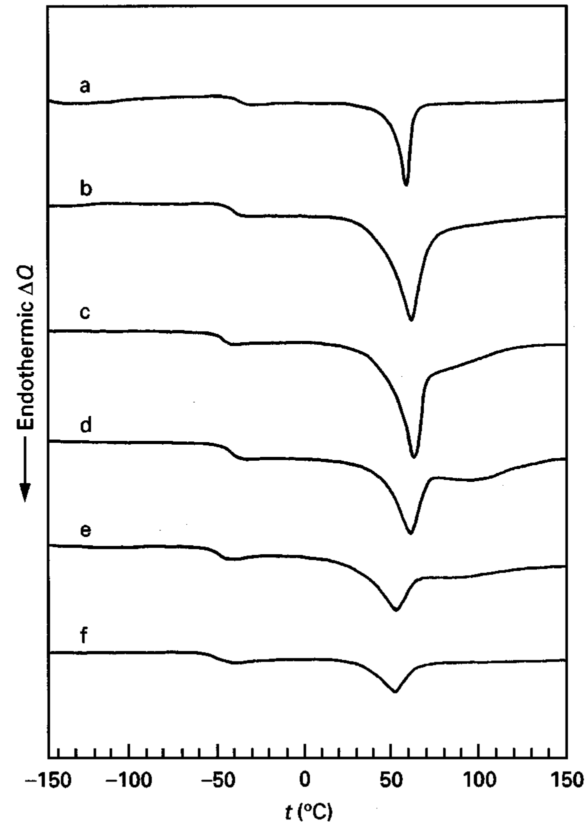

Figure 10 Differential scanning calorimetry thermograms of five PEO–$LiClO_4$–NPANI electrolytes with various [AN unit]/[EO unit] ratios. Curve b, 0.0012; curve c, 0.0022; curve d, 0.0043; curve e, 0.0059; curve f, 0.0118. The original PEO–$LiClO_4$ electrolyte without NPANI (curve a) is also shown for comparison.

the disintegration of the original crystalline PEO phase.

The differential scanning calorimetry thermograms of the PEO–$LiClO_4$–NPANI electrolyte films with different contents of NPANI are indicated in Fig. 10. Both T_g and T_m fluctuate slightly with the NPANI addition. The NPANI addition decreases the endothermic peak at T_m, i.e. the enthalpy of melting, ΔH_m. This behaviour shows the disintegration of the original crystalline PEO phase due to the NPANI addition, as expected from the change in the X-ray diffraction peaks in Fig. 9.

4. Conclusions

It is clear from this study that NPANI is an effective additive to enhance the electrical conductivity of the PEO–$LiClO_4$ electrolyte. The electrical conductivity abruptly increases with increasing NPANI addition, and the conductivity is about one order higher than that of the original PEO–$LiClO_4$ electrolyte (the highest conductivity at room temperature is 6.61×10^{-5} S cm^{-1}). Both the Arrhenius plot of the conductivity of the PEO–$LiClO_4$–NPANI electrolyte and the low possibility of conductivity of the PEO–NPANI without $LiClO_4$ exclude electronic conductivity of NPANI in the electrolyte. In other words, NPANI promotes ion transport in the electrolyte.

From the X-ray photoelectron spectra of the electrolyte films, the absorption spectra of the NPANI in the electrolytes and the electrical conductivity of each PEO–NPANI electrolytes containing different anions, a proposed mechanism for the enhanced ion transport in the PEO–$LiClO_4$–NPANI electrolyte is strongly suggested as follows.

1. The bond energy of $LiClO_4$ is weakened by the electrostatic attraction of the oxygen atoms of the PEO polymer chain, and the ClO_4^- ions become mobile. This Li^+ attraction occurs strongly in NPANI because NPANI has conjugated π electrons.

2. The positively charged nitrogen atoms are electronically stabilized by the π electrons.

3. When NPANI is added, the NPANI polymer chains become entangled in the PEO polymer chains. The Li^+ attraction of the nitrogen atom of the NPANI polymer chain is smaller than that of the oxygen atom of the PEO polymer chain, and the ion–dipole interaction takes place effectively. In the PEO–NPANI electrolyte, therefore, the transport of ClO_4^- is greatly promoted.

Acknowledgements

This work was supported in part by a Grant-in-Aid for Scientific Research 07750903 from the Ministry of Education, Science and Culture of Japan. We thank Mr H. Tang and Dr A. Kitani of Hiroshima University for the measurements of the X-ray photoelectron spectra.

References

1. P. V. WRIGHT, *Brit. Polym. J.* **7** (1975) 319.
2. K. M. ABRAHAM and M. ALAMGIR, *J. Electrochem. Soc.* **137** (1990) 1658.
3. M. B. ARMAND, J. M. CHABANGO and M. J. DUCLOT, "Fast ion transport in solids" (North-Holland, Amsterdam, 1979) p. 131.
4. M. WATANABE, M. RIKUKAWA, K. SANUI, N. OGATA, K. KATO, T. KOBAYASHI and Z. OHTAKI, *Macromolecules* **17** (1984) 2902.
5. M. WATANABE, M. TOGO, K. SANUI, N. OGATA, T. KOBAYASHI and Z. OHTAKI, *ibid.* **17** (1984) 2908.
6. C. K. CHIANG, G. T. DAVIS, C. A. HARDING and T. TAKAHASHI, *ibid.* **18** (1985) 825.
7. H. CHERADAME, J. L. SOUQUET and J. M. LATOUR, *Mater. Res. Bull.* **15** (1980) 1173.
8. A. KILLIS, J. F. LENEST, H. CHERADAME and A. GANDINI, *Makromol. Chem.* **183** (1982) 2835.
9. M. WATANABE, K. SANUI, N. OGATA, T. KOBAYASHI and Z. OHTAKI, *J. Appl. Phys.* **57** (1985) 123.
10. P. M. BLONSKY, D. F. SHRIVER, P. AUSTIN and H. R. ALLCOCK, *J. Amer. Chem. Soc.* **106** (1984) 6854.
11. K. NAGAOKA, H. NARUSE, I. SHINOHARA and M. WATANABE, *J. Polym. Sci., Polym. Lett. Eds* **22** (1984) 659.
12. D. W. XIA, D. SOLTZ and J. SMID, *Solid State ionics* **14** (1984) 221.
13. N. KOBAYASHI, M. UCHIYAMA, K. SHIGEHARA and E. TSUCHIDA, *J. Phys. Chem.* **89** (1985) 987.
14. M. WATANABE, S. NAGANO, K. SANUI and N. OGATA, *Solid State Ionics* **18** (1986) 338.
15. K. MOTOGAMI, M. KONO, S. MORI, M. WATANABE and N. OGATA, *Electrochim. Acta* **37** (1992) 1725.
16. M. KONO, K. FURUTA, S. MORI, M. WATANABE and N. OGATA, *Polym. Adv. Technol.* **4** (1993) 85.
17. W. WHANG, L. YANG and Y. FAN, *J. Appl. Polym. Sci.* **54** (1994) 923.
18. J. LI and I. M. KHAN, *Macromolecules* **26** (1993) 4544.
19. A. G. MACDIARMID, J. CHIANG, M. HALPERN, W. HUANG, N. L. D. SOMASIRI, W. WU and S. I. YANIGER, *Mol. Cryst. Liquid Cryst.* **121** (1987) 173.
20. A. ANDREATTA, Y. CAO, J. CHIANG, A. J. HEEGER and P. SMITH, *Synth. Metals* **26** (1988) 383.
21. M. L. WILLIAMS, R. F. RANDEL and J. D. FERRY, *J. Amer. Chem. Soc.* **77** (1955) 3701.
22. A. KITANI, J. YANO and K. SASAKI, *J. Electroanal. Chem.* **209** (1986) 227.
23. E. M. GENIÈS and M. LAPKOWSKI, *ibid.* **220** (1987) 67.

Received 26 June 1997
and accepted 3 March 1998